Materials Science & Engineering A 640 (2015) 385–393

Contents lists available at ScienceDirect

Materials Science & Engineering A

journal homepage: www.elsevier.com/locate/msea

Dynamic behavior of a 6069 Al alloy under hot compression

Feng-jun Zhu [a], Horng-yu Wu [b,*], Shyong Lee [a], Ming-chieh Lin [b], Delphic Chen [c]

[a] Department of Mechanical Engineering, National Central University, Jhongli 320, Taiwan
[b] Department of Mechanical Engineering, Chung Hua University, HsinChu 300, Taiwan
[c] Research Center for Physical Properties and Microstructure of Metals, National Sun Yat-Sen University, Kaohsiung 804, Taiwan

ARTICLE INFO

Article history:
Received 7 May 2015
Accepted 7 June 2015
Available online 10 June 2015

Keywords:
6069 Al alloy
Strain-hardening
Dynamic recovery
Continuous dynamic recrystallization
Relative softening

ABSTRACT

The high temperature deformation behavior of a 6069 Al alloy was examined on a Gleeble 3500 thermal–mechanical simulation machine at temperatures ranging from 300 °C to 550 °C and strain rates varying between 0.001 s^{-1} and 10 s^{-1}. The strain-hardening and dynamic softening mechanisms of the alloy were analyzed. Strain-hardening behavior was investigated using Kocks–Mecking type plots. Stage III hardening behavior occurred immediately after yielding under the deformation conditions performed in this study. Microstructural evolution analysis indicated that the softening mechanism at high strain rates or low temperatures proceeded via dynamic recovery. The net flow stress required for the onset of dynamic recovery increased with increasing strain rate or decreasing temperature. Partial dynamic recrystallization enhanced the softening effect at high temperatures with low strain rates. The microstructural evolution analyzed via electron backscatter diffraction showed that the operating mechanism of dynamic recrystallization was related to continuous dynamic recrystallization. A relative softening factor was used to quantify the effect of flow softening. The variations in the relative softening value with strain may be associated with hot deformation conditions, in which the flow stress behavior correlated with different microstructures and dynamic softening mechanisms.

1. Introduction

The Al alloy AA6069 is widely used in impact airbag components, light weight bicycle frames, and high-pressure seamless gas containers because of its strength, extrudability, and corrosion resistance with low cost [1,2]. The mechanical properties of this alloy have been comprehensively explored [1–6]; however, its hot deformation behavior has yet to be comprehensively analyzed [7].

Hot deformation significantly changes the microstructure of Al alloys and contributes to hot workability, which is sensitive to process conditions [8–11]. Hot deformation behavior is related to strain-hardening and dynamic softening mechanisms. Dynamic recovery (DRV) and dynamic recrystallization (DRX) are important dynamic softening mechanisms for characterizing microstructures during the hot deformation of Al alloys [12–16]. Changes in the microstructure of Al alloys during hot deformation also influence their flow behavior, which is associated with their deformation mechanism and softening effect. Whether only DRV or DRV with partial DRX is observed during hot working depends on the temperatures and strain rates involved. Some metals and alloys only undergo DRV and not DRX. Materials that do not dynamically recrystallize exhibit rapid recovery rates and thus do not develop a dislocation density and configuration sufficient to nucleate and drive recrystallization. These materials include high-stacking-fault energy (SFE) face-centered cubic (FCC) metals, such as Al [17]. However, Al alloys undergo DRX, and discontinuous dynamic recrystallization (DDRX), continuous dynamic recrystallization (CDRX), and geometric dynamic recrystallization (GDRX) have been proposed as their mechanisms [8,10,18–20]. CDRX is a recovery-dominated process that involves the progressive increase in boundary misorientation and the conversion of low angle boundaries into high angle boundaries [8,11,15,16,18,20]. Gradual softening in the flow curve is observed in this type of recrystallization. DDRX is characterized by nucleation through the bulging of serrated grain boundaries; this phenomenon typically causes a significant softening effect on the flow curve [15,16,20]. The basic mechanism of GDRX is that the grains are increasingly flattened during deformation until the starting high angle boundaries are serrated as a result of subgrain boundary formation. The points of the serrations eventually come into contact with one another, where the grain boundaries begin to “pinch off” and form new grains with high misorientation [10,15,16,18,19].

The hot deformation characteristics of a 6069 Al alloy must be understood to control its microstructural evolution during hot working and to optimize its plastic deformation processes. In this study, the dynamic behavior of a homogenized 6069 Al alloy cast

* Corresponding author. Fax: +886 3 5186521.
E-mail address: ncuwu@chu.edu.tw (H.-y. Wu).

http://dx.doi.org/10.1016/j.msea.2015.06.026
0921-5093/

ingot was investigated using hot compression tests. The flow curves were examined with respect to the temperature and strain rate, and the hardening and softening mechanisms were analyzed. The microstructural evolution of the 6069 Al alloy during hot deformation was investigated to understand its various dynamic softening mechanisms under different deformation conditions.

2. Materials and experimental procedures

The experimental material was a homogenized 6069 Al alloy cast ingot with a chemical composition of Al–1.23Mg–0.78Si–0.74Cu–0.15Cr–0.12V (wt%). Cylindrical specimens 6 mm in diameter and 9 mm in height were prepared with their axes aligned along the centerline of the ingot. Fig. 1 shows the initial microstructure of the homogenized specimen. Hot compression tests were conducted on a Gleeble 3500 thermal–mechanical simulation machine at temperatures ranging from 300 °C to 550 °C, and constant strain rates varying between 0.001 s^{-1} and 10 s^{-1}. The specimen temperature was measured with a thermocouple spot welded at the central region on the specimen surface. Before being subjected to hot compression, the specimens were heated at a rate of 5 °C/s by the thermocouple feedback-controlled AC current until the deformation temperature was reached. This deformation temperature was then kept constant for 3 min to eliminate thermal gradients and to ensure the uniform temperature of the specimens. The stimulator was equipped with a control system to induce the exponential decay of the actuator speed to achieve a constant strain rate. The specimens were lubricated with graphite to reduce friction at the punch–specimen interface. The initial height of the specimen was subsequently reduced to 50%, corresponding to a true strain of approximately 0.7. The specimens were immediately water quenched after hot compression. Some selected samples were also deformed to different true strains of 0.1, 0.3, and 0.5, followed by water quenching, to investigate their microstructural evolution during deformation. The true stress–strain curves were constructed using the load-stroke data obtained from the compression tests.

The specimens used for microscopic examination were prepared using conventional metallographic techniques. The polished specimens were etched for approximately 90 s in Keller's reagent comprising 2.5 mL of HNO_3, 1.5 mL of HCl, 1.0 mL of HF, and 95 mL of water. The microstructures were observed under an optical microscope. The microstructural evolution analysis was carried out using electron backscatter diffraction (EBSD) technique.

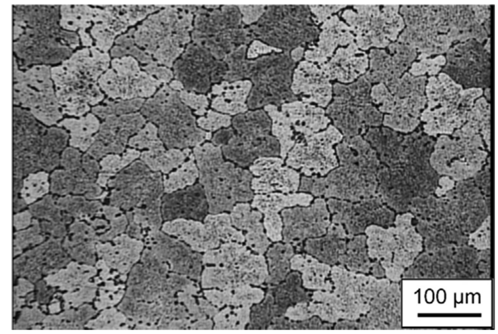

Fig. 1. Optical image of the initial microstructure of the 6069 Al alloy.

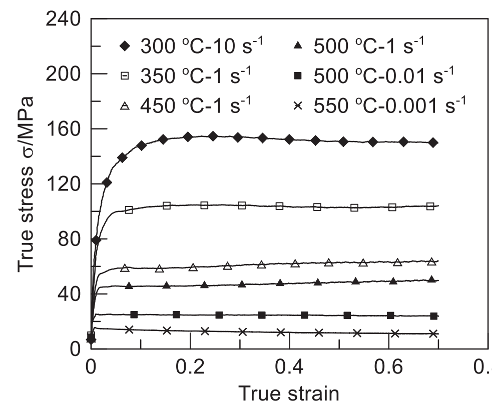

Fig. 2. Typical true stress–true strain curves of 6069 Al alloy deformed at various conditions.

3. Results and discussion

3.1. Flow behavior

The typical true stress–true strain curves obtained at various deformation conditions are shown in Fig. 2. The flow stress level decreases with increasing temperature and decreasing strain rate. In general, the flow curves exhibit a flow behavior with dynamic softening. The flow stress increases because of strain-hardening at the onset of plastic deformation. The rate of increase in flow stress decreases with increasing strain. The flow behavior is significantly influenced by the deformation conditions. Apparent hardening followed by softening was observed at low temperatures or/and high strain rates. At high temperatures or/and low strain rates, a dynamic equilibrium between hardening and softening occurs at the very beginning of deformation. The strain corresponding to the peak stress increases with increasing strain rate and/or decreasing deformation temperature. This relation is attributed to the high hardening effect at the initial stage of deformation. The flow stress curves can be divided into three typical cases, which should be closely associated with dynamic softening mechanisms. In the first case, the flow stress initially increases, reaches the peak value, and then decreases continuously with increasing strain under the deformation conditions of 500 °C with 0.01 s^{-1} and 550 °C with 0.001 s^{-1}. This occurrence reveals that the rate of dynamic softening is higher than that of strain-hardening. In the second case, the flow stress increases, reaches the peak value, and then arrives at a near steady-state value under the deformation conditions of 300 °C with 10 s^{-1} and 350 °C with 1 s^{-1}. This event implies that a dynamic equilibrium between the strain-hardening and dynamic softening is achieved. In the third case, the flow stress continuously increases with increasing strain after the early stage of deformation under the conditions of 450 °C with 1 s^{-1} and 500 °C with 1 s^{-1}. This result shows that the rate of strain-hardening is higher than that of dynamic softening.

3.2. Strain-hardening behavior

The Kocks–Mecking type plot of the strain-hardening behaviors tested at various deformation conditions is depicted in Fig. 3. The plot is derived from the data of the stress–strain curves, and it illustrates the relationship between the strain-hardening rate Θ ($d\sigma/d\varepsilon$) and the net flow stress ($\sigma - \sigma_y$), where σ_y is the (0.2% off-set) yield strength and σ is the total flow stress, during hot deformation under various deformation conditions. The figure particularly shows that the strain-hardening of stage III behavior with decreasing Θ occurs immediately after yielding for the hot compression of the 6069 alloy [21]. In general, an initial Θ value decreases with increasing temperature and decreasing strain rate. Moreover, the decreasing rate of Θ with net flow stress increases with increasing temperature and decreasing strain rate. Fig. 3 also shows that a lower decreasing rate of Θ with net flow stress, which is similar to the strain-hardening behavior in stage IV [21–